International Journal of Innovative Research in Engineering
Volume 1, Issue 2 (September-October 2020), PP: 53-62
www.theijire.com

ANFIS Based Adaptive Gliding Mode Control of a Detached Single-Phase Micro grid

J SARAVANAN [1], SELVARAJ SIVASAKTHI.S[2]
[1]*PG Student,. Department of Electrical and Electronics Engineering, Dayanand Sagar College of Enginnering ·India*
[2]*Assistant Professor, Department of Electrical and Electronics Engineering, Dayanand Sagar College of Enginnering India*

How to cite this paper: J SARAVANAN [1], SELVARAJ SIVASAKTHI.S[2] , ANFIS Based Adaptive Gliding Mode Control of a Detached Single-Phase Micro grid. IJIRE-V1I2, 53-62

Abstract*-This paperpresents an ANFIS based adaptive sliding mode control (ASMC) of a standalone single phase micro grid system. The proposed micro grid system integrates a micro-hydro turbine driven single-phase two winding self- excited induction generator (SEIG) with a wind driven permanent magnet brushless DC (PMBLDC) generator, solar photo- voltaic (PV) array and a battery energy storage system (BESS). These renewable energy sources are integrated using a single-phase voltage source converter (VSC). The ASMC based control algorithm is used to estimate the reference source current which controls the single-phase VSC and regulates the voltage and frequency of the microgrid in addition to harmonics current mitigation. The adaptive sliding mode control with ANFIS is used to maintain the energy balance among wind, micro-hydro, solar PV power and BESS, which controls the frequency of standalone microgrid. Simulation results from MATLAB/SIMULINK of the proposed microgrid shows that the grid voltage and frequency are maintained constant while the system is following various changes in dynamic state such as sudden change in wind speed, changes in solar insolation level and changes in loads.*

Index terms*—Adaptive Neuro Fuzzy interface System, Battery Energy Storage System(BESS), Renewable Energy Sources, single-phase SEIG.*

I. INTRODUCTION

The demand for power is ever-increasing. Use of fossil fuels i.e. gas, coal, oil etc. in producing power is also increasing. Still, there are over 1.5 billion people over the world deprived of access of electricity living mostly in remote areas. The source of electricity in those remote islands and villages is diesel generator. This is both costly and hazardous for the environment due to the global warming. Renewable energy resources like wind and solar energy are getting popularity for these reasons. Two or more renewable energy resources can be utilized in a hybrid renewable energy system (HRES) which can work as a standalone or grid connected system. A hybrid renewable energy system offers better quality in terms of reliability compared to single source based system. This is due to the fact that one power source can supply power to the load when other sources are either generating low or no power. The selection of renewable resources in HRES depends on the particular location. In this paper a wind-solar HRES is considered. Wind and solar combination is most promising source of generating energy primarily due to their complementary nature advantage. Wind power generation could be low in time when solar power generation is in its peak. On the other hand, the wind is often stronger in seasons when there is less solar irradiance. Wind and solar energy are unpredictable in nature, as they depend on climate condition. To improve the reliability of a wind-solar hybrid system other sources like battery storage, single-phase SEIG can also be integrated [1].

The architecture of electric power systems and their energy or power management are designed and adapted in realistic conditions to optimally provide electric power to consumers in all modes of production and consumption. Originally designed to supply electricity to consumers from nuclear, thermal, or hydraulic power plants, the architecture of classical electric power systems will undergo major changes in the future, including the arrival of numerous economic actors and low-power generation units (co-generation units, generators based on renewable or non-conventional energy sources) not interfaced with a supervisory position, leading to profound changes in the management of the current electric power systems including technical, environmental, and financial variables. An evolution towards new architectures well adapted to these

recent modes of dispersed production has then to be imagined for future times [14]. The definition of Microgrids, such as those already present in islands or isolated areas, could be a response to this development.

Microgrids have two essential intrinsic characteristics which make them a major interest for the development of the electric power systems of the future:

- The proximity between local electricity production and different consumers leads to an immediate minimization of transportation losses;
- The distinctive autonomous operational capability of microgrids has brought in higher reliability measures in supplying power demands when the utility grid is not available.

The concept of microgrid is most interesting for successful dealing with the challenges in the integration of renewable energy sources [2]-[4]. A microgrid is having capability to operate in both standalone and grid tied modes operation depending upon the design of suitable control scheme [5]. The various derived forms of the microgrid such that virtual power plant, cognitive microgrid and active distribution system can be studied as a main constituent of smart grid [7], [8], [10]. In grid tied microgrid, the main grid supplies the deficit power and absorbs the surplus power in order to maintain power balance which in turn regulates the system frequency.

The future power grids will thus be multi-converter and multi-source systems, particularly with the massive insertion of Renewable energy sources and storage devices interfaced with power-electronic converters, and the current trend favoring electricity as energy vector [6]. This concerns especially microgrids and future smart grids (at distribution level and even at transportation level). Electric power systems, integrating microgrids, must therefore be partially or completely re-designed in order to integrate these new intermittent sources that could negatively affect quality of power supplied due to their very low short-circuit power [11]-[13]. Moreover, the development of power-electronic interfaces can potentially induce unstable operation due to dynamic and harmonic interactions generated by the converters[15]. Uncertainties associated with weather conditions or parametric sizing play also a major role in the lack of microgrids reliability, which induces oversizing of different components within the microgrids such as storage devices [9]. Research problems associated with microgrids concern consequently the development of optimal control strategies allowing maximizing power quality, securing supply, maximizing efficiency, performance, reliability, and costs associated with the system [12].

II. System Configuration Of The Single-Phase Microgrid

The ASMC algorithm provides a robust and adaptive control of system frequency and voltage with good dynamic and steady state response, which is the main requirement of a good standalone microgrid as reported by IEEE-PES Task Force on microgrid control. The reported single-phase SEIG is investigated by many researchers for bio energy and small hydro driven systems but the benefits of this machine are not fully exploited for microgrid system (fearing the complications of nonlinear relationship in frequency, magnetizing reactance and speed of single phase SEIG). SEIGs have many advantages over other generators, like simple, brushless, low unit cost, low maintenance, high power/weight ratio, absence of DC excitation etc. In the proposed system the governor-less control of small hydro uncontrolled turbine driven SEIG and wind driven PMBLDC generators, reduces the overall cost and size of the generators significantly. It also makes the system frequency independent of the mechanical inertia of turbine generator.

The block diagram of proposed single-phase microgrid is depicted in Fig..1. This microgrid consists of an unregulated micro-hydro turbine driven single-phase two winding SEIG (Self-Excited Induction Generator), a wind turbine driven PMBLDC (Permanent Magnet Brushless DC) generator, solar PV (Photovoltaic) array and a BESS. Conceptually, the single-phase SEIG is only the AC generating source in this microgrid, which directly caters the load whereas remaining two generating sources are connected to the load through a voltage source converter (VSC). It converts the DC power generated by PMBLDC generator and solar PV array into AC power when the power generated from SEIG is less than the load. The solar PV-array, wind turbine driven PMBLDC generator and BESS are connected at the DC bus of the VSC.

All these three energy sources supply only the real power to the system. They do not participate in any reactive power transaction with the system. When the total real power generated by the SEIG, PMBLDC generator and solar PV-array is less than the load, then the BESS compensates the additional real power demand of the load. The VSC converts the DC power supplied by the BESS into the AC power to make it suitable for single-phase load connected at AC side of microgrid.

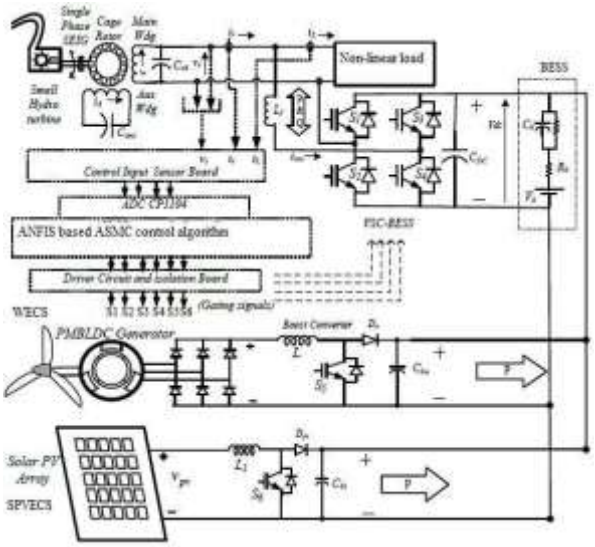

Fig.1. System Configuraion of the single phase microgrid

III. Control Algorithm For ANFIS Based ASMC of The Microgrid

The block diagram of proposed ASMC algorithm is shown in Fig. 2. It is well known that the SEIG system requires an adjustable reactive power under varying load conditions to maintain the PCC voltage at reference value. The quadrature constituent of microgrid AC voltage is estimated and generated using frequency estimation and phase shifting (FEPS) block. The in-phase part of reference source current is responsible for frequency control of the system and power balance among SEIG, PMBLDC generator, solar PV-array, battery and the load. In proposed ASMC control algorithm, an adaptive filter is used to extract the amplitude of fundamental active and reactive power constituents of load current.

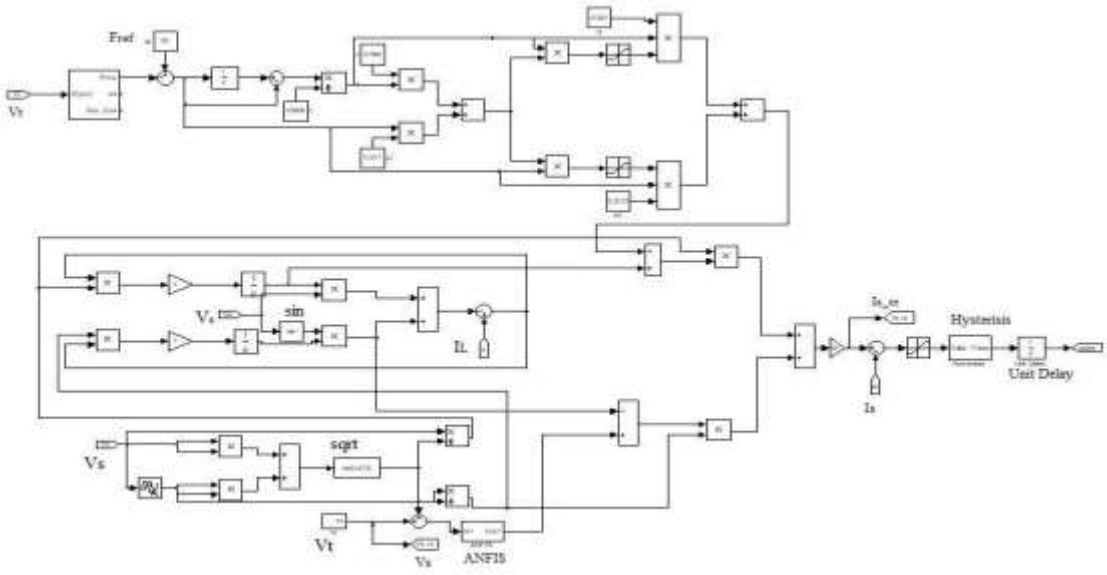

Fig:2. Control algorithm for ANFIS based adaptive sliding mode control (ASMC).

The proposed control algorithm is a combination of two control loops. First loop controls its voltage by injecting an adjustable reactive power and other loop maintains active power balance among various energy elements in the microgrid. The Perturb and Observe (P & O) control algorithm is used for sensor less control for MPPT of PMBLDC generator based wind energy conversion system. A boost converter is connected at the output of diode bridge rectifier. This converter is controlled using P & O algorithm to extract maximum power from the wind generating system. An incremental conductance based control algorithm is used to extract maximum power generated from solar PV array.

IV. RESULTS AND DISCUSSION

The effect of change in insolation level and step change in wind speed and load are taken into consideration to verify the dynamic performance of the proposed control. All the MATLAB simulation results of the dynamic performance of the system are presented in this chapter.

CASE-1: DYNAMIC PERFORMANCE OF PROPOSED MICROGRID AT A STEP CHANGE IN SOLAR INSOLATION LEVEL

The response of microgrid following a step change in solar insolation level is demonstrated in Figs. 3.1(a), 3.1(b) and 3.1(c). A step increase in solar PV-array output current (channel 1 of result shown in Fig. 3.1(b)) has been observed while the system is following a step increase in insolation level at 0.2 sec from 1000 to 5000 w/m^2.

The dynamic performance of SEIG current is shown in Fig. 3.1(a), while the system is following a step increase in insolation level. Fig. 3.1(a) shows that the step change in solar insolation level does not cause any change or disturbance in the system voltage and SEIG current. It proves that proposed controller maintains the power balance under a dynamic situation arose due to step increase in solar insolation level which in turn increases the solar PV-array output current. The total generated power from all three renewable sources (micro-hydro, wind and solar PV array) becomes more than load. Therefore, surplus power is diverted to the battery in order to control the system frequency. The dynamic performance of the system voltage, SEIG current, solar PV-array current and battery current while the system is following a step decrease in insolation level at 0.4 sec from 5000 to 1000 w/m^2, are demonstrated in Fig. 3.1(b). It is observed from test results shown in Fig. 3.1(b) that the step decrease in insolation level causes a decrease the solar PV-array current with the same slope and it subsequently decreases the battery current but it does not disturb the system AC voltage, load current or system frequency. The battery current goes from charging to discharging mode in order to regain the power balance in the system as shown in Fig. 3.1(b). Simulation results show that the system frequency and voltage are maintained constant during this dynamic condition.

Fig. 3.1(b) demonstrates the directional change of the battery current from discharging to charging mode in response to a step increase in solar PV-array output current. This balance of power among the various energy sources is achieved using frequency control loop of the proposed ASMC algorithm.

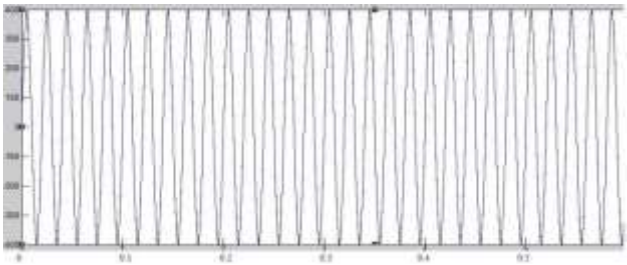

X-axis: time in sec; Y-axis: voltage (v) in volts

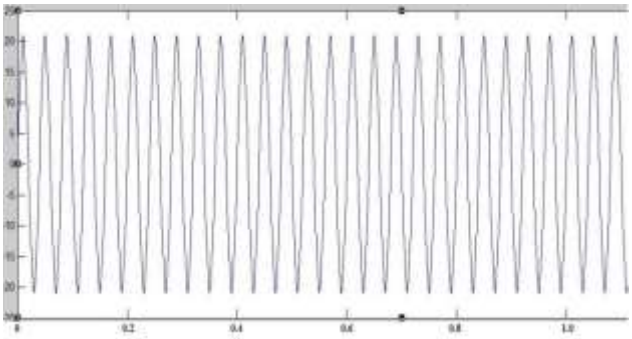

X-axis: time in sec; Y-axis: current (I) in amps

Fig.3.1 (a): Dynamic performance of the V_s, I_s while the system is following a step change in insolation level.

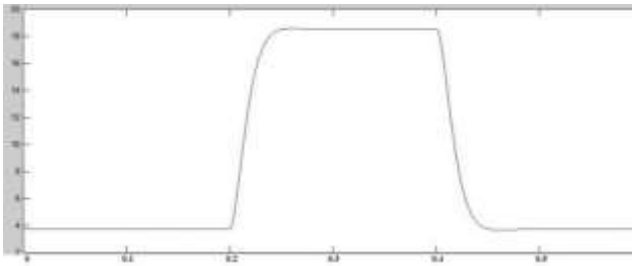

X-axis: time in sec; Y-axis: current (I) in amps

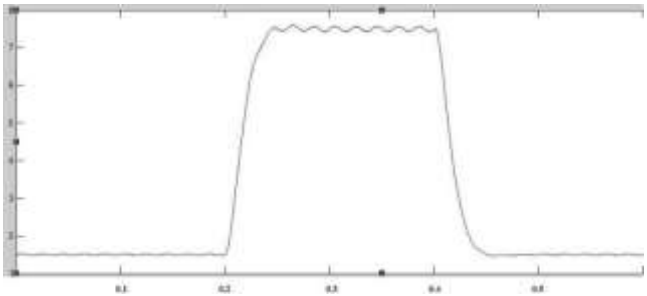

X-axis: time in sec; Y-axis: current (I) in amps

Fig.3.1 (b): Dynamic performance of the Ipvand$I_{battery}$, while the system is following a step increase in insolation level.

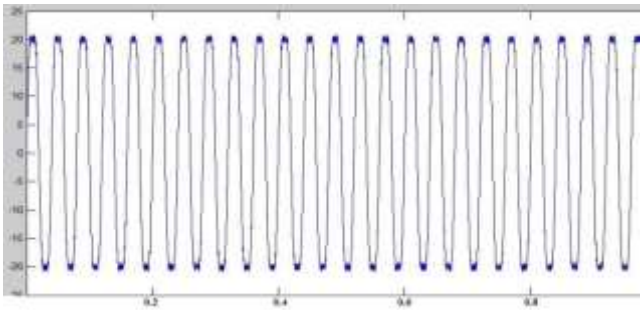

X-axis: time in sec; Y-axis: current (I) in amps

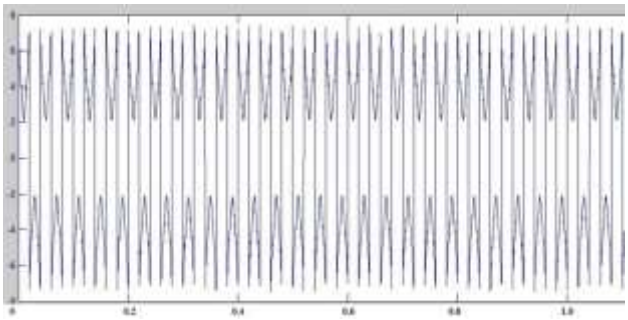

X-axis: time in sec; Y-axis: current (I) in amps

Fig.3.1(c): Dynamic performance of the I_L, I_{VSC} while the system is following a step change in insolation level.

The above fig. shows that load current and VSC current are not disturbed by the changes in insolation level. Simulation results (Figs. 3.1(a) to 3.1(c)) show that in response to this step change in solar PV-array output current, the controller increases the charging current of the battery to divert the surplus generated power to BESS in order to control the system frequency

CASE-2: DYNAMIC PERFORMANCE OF MICROGRID, UNDER A STEP CHANGE IN WIND SPEED

The effect of a step change in the wind speed and consumer load on various other power quality parameters like system voltage, VSC current and load current, is considered to evaluate the dynamic performance of proposed microgrid.

The dynamic response of load current, VSC current are shown in Fig. 3.2(a) while the system is following a step change in wind speed (i.e. at 0.2 sec it increases from 7 m/s to 12 m/s) . A step increase in PMBLDC generator current is observed in Fig. 3.2(b) while microgrid is following a step increase in wind speed. Test results shown in Fig. 3.2(a) to Fig. 3.2(c) show the system response to step increase in wind speed. The controller increases the battery charging current to divert the surplus generated power to the battery in order to control the system frequency.

The dynamic response of system AC voltage, SEIG current, PMBLDC generator current and battery current while the system following a step decrease in wind speed(i.e. at 0.4 sec it decreases from 12 m/s to 7 m/s), is demonstrated in Fig.3.2(b), 3.2(c). A step decrease in PMBLDC generator current (in response to the step decrease in wind speed) does not cause any disturbance in the SEIG current and system AC voltage as shown in Fig. 3.2(c).

Fig. 3.2(b) demonstrates the directional change of battery current from discharging to charging mode in response to a step increase in PMBLDC generator current. This balance of power among the various energy sources is achieved using frequency loop of the control algorithm. The step increase in wind speed and PMBLDC generator current does not cause any disturbance or change in load current, as demonstrated in Fig. 3.2(a). It can be observed from test results shown in Fig. 3.2(c) that a step decrease in wind speed causes a decrease in the PMBLDC output current with the same slope and it subsequently decreases the battery current.

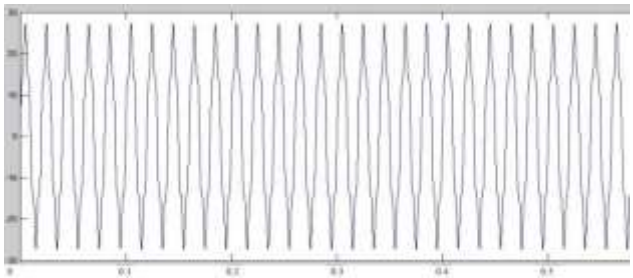

X-axis: time in sec; Y-axis: current (I) in amps

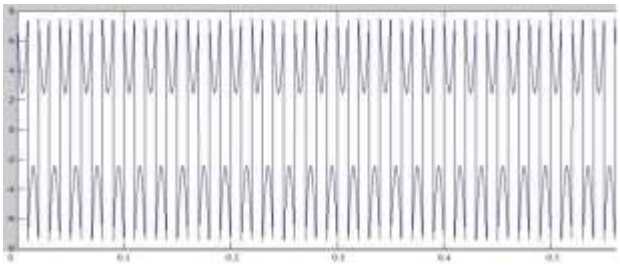

X-axis: time in sec; Y-axis: current (I) in amps

Fig.3.2 (a): Dynamic response of I_L, I_{VSC} while the system is following a step change in wind speed.

Test results shown in Figs. 3.2(a) show that total generated power from all three renewable sources (micro-hydro, wind and solar PV array) becomes more than that of load, while the system is following a step increase in wind speed**.** Therefore, battery charging current increases to divert surplus power to the battery in order to control the system frequency.

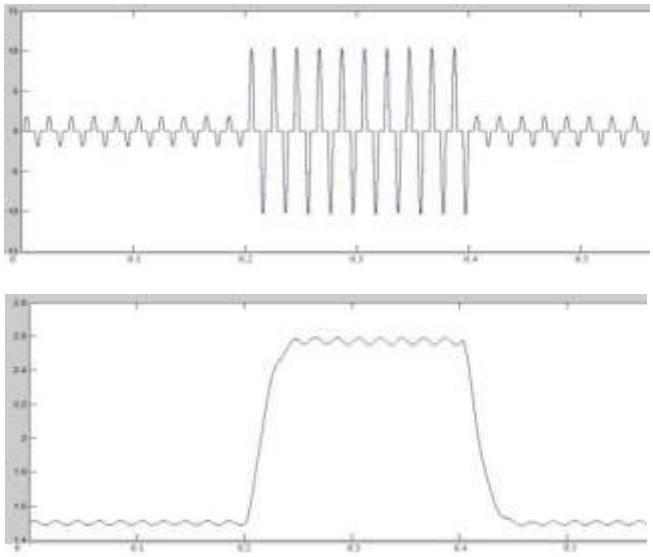

X-axis: time in sec; Y-axis: current (I) in amps

Fig.3.2 (b): Dynamic response of $I_{pmbldc}$and $I_{battery}$ while the system is following a step increase in wind speed.

As shown in the above fig. when the wind speed increases at 0.2 sec from 7 m/s to 12 m/s the PMBLDC current increases which in turn charges the battery, so battery current increases with the same slope as shown. At 0.4 sec the wind speed comes down from 12 m/s to 7 m/s, so the PMBLDC current decreases and the battery also discharges as shown. While system is following a step decrease in wind speed, the battery enters discharging mode from charging mode in order to regain the power balance in the system as shown in Fig. 3.2(b).

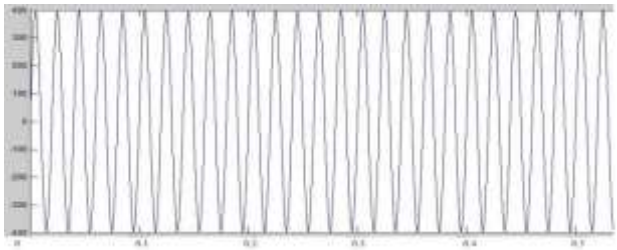

X-axis: time in sec; Y-axis: voltage (v) in volts

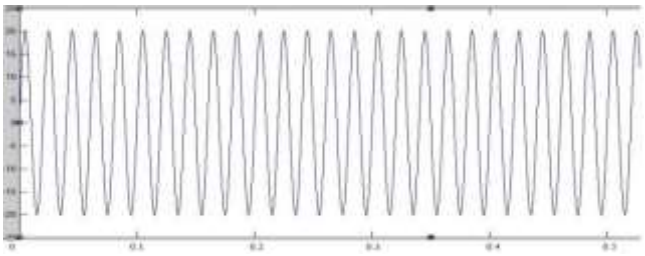

X-axis: time in sec; Y-axis: current (I) in amps

Fig.3.2 (c): Dynamic response of V_s, I_s, while the system is following a step increase in wind speed.

A step decrease in wind speed does not disturb the power quality parameters of the microgrid such as system frequency and voltage. It also does not cause any variation in the SEIG output current and load current. It can be clearly observed from Fig. 3.2(c) that the BESS entering the discharging mode from the charging mode in response to a step decrease in wind speed to control the system frequency and to maintain the balance of power among various generators and BESS. A step decrease in wind speed does not disturb the power quality parameters of the microgrid such as system frequency, voltage. It also does not cause any fluctuation in the SEIG voltage, current and load current. Test results shown in Figs. 3.2(a) to 3.2(c) prove the ability of the proposed control algorithm to balance the power among the various sections of the system while the wind speed is fluctuating.

CASE-3: DYNAMIC PERFORMANCE OF THE MICROGRID, WHILE IT FOLLOWING A STEP CHANGE IN LOAD:

The dynamic response of the load current, VSC current, SEIG output voltage and system frequency while system is following a step change in load is demonstrated in Fig. 3.3a) and 3.3b) respectively.

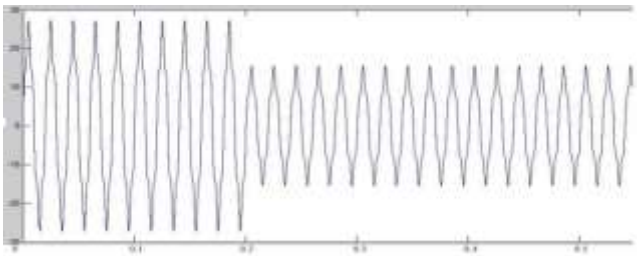

X-axis: time in sec; Y-axis: current (I) in amps

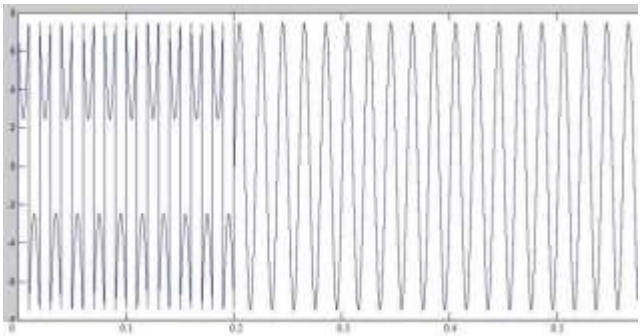

X-axis: time in sec; Y-axis: current (I) in amps

Fig.3.3 a): Dynamic response of I_{load} and I_{vsc} following a step change in load.

In the Simulink model of the load there are two switches S1 and S2. Initially S1 is closed and S2 is open. At 0.2 sec S1 is opened and S2 is closed, changes in the load current and VSC current at this instant are as shown in the above fig.

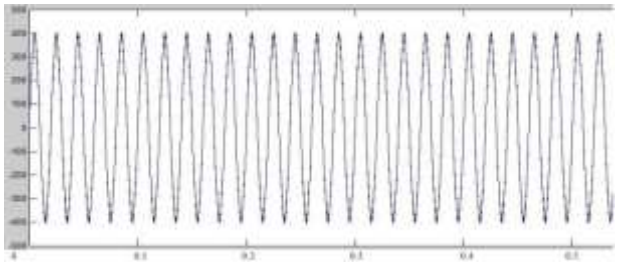

X-axis: time in sec; Y-axis: voltage (v) in volts

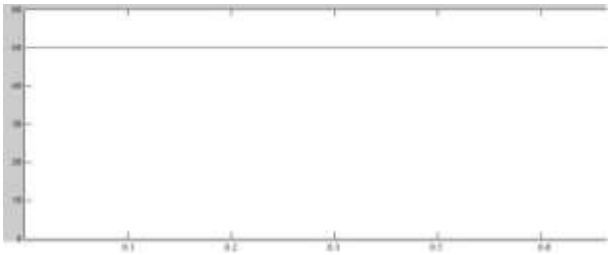

X-axis: time in sec; Y-axis: frequency in hertz

Fig.3.3 b): Dynamic response of Vs and system frequency following a step change in load.

In this dynamic condition, the proposed control re-estimates the revised harmonic and fundamental reactive power need of the SEIG and load as well as active power need of the load with an excellent dynamic response. Here the control revises the switching pattern for VSC to compensate the new reactive and active powers need of the system in order to regulate system voltage and frequency, respectively. Fig. 3.3.b) shows that microgrid voltage and frequency are restored to their rated value immediately in response to sudden change in load.

V. CONCLUSION

The proposed ANFIS based standalone microgrid has integrated three main renewable energy sources micro-hydro SEIG, solar PV, and wind energy. Simulation results from MATLAB/SIMULINK have proven that the ANFIS based ASMC algorithm has been effective and has good control of the microgrid voltage and frequency. The grid voltage and frequency are maintained constant while the system is following various changes in dynamic state such as sudden change in wind speed, change in solar insolation level and changes in load. The proposed control algorithm has also improved the power quality of the microgrid under nonlinear loads and also ensures the optimum utilization of BESS and renewable energy sources.

References

1. U. K. Kalla, B. Singh, and S. S. Murthy, “Normalized adaptive linear element-based control of single-phase self- excited induction generator feeding fluctuating loads,” *IET Power Electron.*, vol. 7, no. 8, pp. 2151–2160, Aug. 2014.
2. U. K. Kalla, B. Singh and S. S. Murthy, "Enhanced Power Generation From Two Winding Single-Phase SEIG Using LMDT-Based Decoupled Voltage and Frequency Control," in *IEEE Transactions on Industrial Electronics*, vol. 62, no. 11,pp. 6934-6943, Nov. 2015.
3. U. K. Kalla, B. Singh and S. S. Murthy, "Adaptive noise suppression filter based integrated voltage and frequency controller for two-winding single- phase self-excited induction generator," in *IET Renewable Power Generation*, vol. 8, no. 8, pp. 2014
4. U. K. Kalla, B. Singh and S. S. Murthy, " Adaptive Sliding Mode Control of Standalone Single-Phase Microgrid Using Hydro, Wind and Solar PV Array Based Generation," in *IEEE Transactions on Industry Applications*, vol. 52, no. 4, pp. 2789-2800, Aug. 2017.
5. D. E. Olivares *et al.*, “Trends in microgrid control,” *IEEE Trans. Smart Grid*, vol. 5, no. 4, pp. 1905–1919, Jul. 2014.
6. J. Rocabert, A. Luna, F. Blaabjerg, and P. Rodríguez, “Control of power converters in AC microgrids,” *IEEE Trans. Power Electron.*, vol. 27, no. 11, pp. 4734–4749, Nov. 2012.
7. D. Pudjianto, C. Ramsay, and G. Strbac, “Virtual power plant and system integration of distributed energy resources,” *IET Renew. Power Gener.*, vol. 1, no. 1, pp. 10–16,Mar.2007.
8. D. Pudjianto, C. Ramsay, and G. Starbac, “Microgrids and virtual power plants: Concepts to support the integration of distributed energy resources,” *Proc. Inst. Mech. Eng. A J.Power Energy*, vol. 222, no. 7, pp. 731–741, 2008.

9. P. Dondi, D. Bayoumi, C. Haederli, D. Julian, and M. Suter, "Network integration of distributed power generation," *J. Power Sources*, vol. 106, nos. 1–2, pp. 1–9, 2002.
10. Katiraei, M. R. Iravani, and P.W. Lehn, "Micro-grid autonomous operation during and subsequent to islanding process," *IEEE Trans. PowerDel.*, vol. 20, no. 1, pp. 248–257, Jan. 2005.
11. *IEEE Standard for Interconnecting Distributed Resources with Electric Power Systems*, 2003, IEEE Std. 1547.
12. R. Zamora and A. K. Srivastava, "Controls for microgrids with storage: Review, challenges, and research needs," *Renewable and Sustainable Energy Reviews*, vol. 14, no. 7, pp. 2009–2018, Sep. 2010.
13. A. Hajimiragha and M. R. D. Zadeh, "Practical aspects of storage modeling in the framework of microgrid real-time optimal control," in *Proc. IET Conf. on Renewable Power Generat. (RPG)*, Sep. 2011, pp. 93– 98.
14. F. Blaabjerg, R. Teodorescu, M. Liserre, and A. V. Timbus, "Overview of control and grid synchronization for distributed power generation systems," *IEEE Trans. Ind. Electron.*, vol. 53, no. 5, pp. 1398–1409, Oct. 2006.
15. A. Timbus, M. Liserre, R. Teodorescu, P. Rodriguez, and F. Blaabjerg, "Evaluation of current controllers for distributed power generation systems," *IEEE Trans. Power Elect.*, vol. 24, no. 3, pp. 654–664, Mar. 2009.